Applied Ocean Research 153 (2024) 104276

Contents lists available at ScienceDirect

Applied Ocean Research

journal homepage: www.elsevier.com/locate/apor

On the value of Fano resonance in wave energy converters☆,☆☆

Andrei M. Ermakov [a,*], Jack L. Rose-Butcher [b], John V. Ringwood [a]

[a] Centre for Ocean Energy Research, Maynooth University, Maynooth, W23 A3HY, Co. Kildare, Ireland
[b] Hanze University of Applied Sciences, Groningen, 9747 AS, Netherlands

ARTICLE INFO

Keywords:
Wave energy converter
Fano resonance
Point absorber
Optimal control
Parametric analysis

ABSTRACT

The article evaluates the potential of the Fano resonance operational principle in wave energy converters (WECs), using a 2-body loosely moored self-referenced WEC as an illustrative example. By leveraging Fano resonance, the point absorber buoy can remain relatively stationary with low loading on mooring lines, serving as an efficient wave energy transmitter while concurrently achieving resonance within the internal power take-off (PTO) system. This arrangement reduces the motion of the point absorber hull, thereby decreasing loads on the WEC structure, mooring lines, and anchors. As a result, operational and structural costs are minimised, further reducing the levelised costs of generated energy. Additionally, by ensuring minimal fluctuations in the WEC, confidence in using traditional linear mathematical models is increased, as commonly employed for WEC performance assessment and control design.

The article presents a resonance study and introduces newly derived solutions in the frequency domain for the proposed operational concept. It analytically demonstrates the viability of employing the Fano resonance operational strategy for WECs, suggesting that this strategy has the potential to compete with traditional methods of wave energy transformation. Furthermore, the insights gained from the study contribute to identifying optimal parameters for a PTO system, as well as optimising the design of the heaving buoy.

1. Introduction

Despite nearly 50 years of research and development in wave energy harvesting technology, a commercially viable device has yet to emerge (Guo and Ringwood, 2021c). The primary obstacle in the realisation of numerous wave energy extraction solutions is the cost of the generated electrical energy which, unfortunately, cannot currently compete with wind and solar energy. The conventional method for evaluating the price of renewable energy is based on the levelised cost of energy (LCoE) (Guo et al., 2023). The LCoE can be succinctly presented as the ratio between the total expenditure on a device (capital and operational costs, or CapEx and OpEx), divided by the power produced over its lifetime:

$$LCoE = \frac{CapEx + OpEx}{Generated\,Power}. \tag{1}$$

While published research and developed prototypes (Giglio et al., 2023; Jahangir et al., 2023; CorPower Ocean, 2023; Wave Star, 2023) offer insights into CapEx, accurate estimates for OpEx remain challenging. Factors driving up the estimated values of both OpEx and CapEx include the high costs of mooring lines, anchors, or any other marine support structures. These elements are vital for device sustainability in harsh marine environments and come with associated maintenance and repair requirements.

In this article, the authors assess a novel operational principle and design for a power take-off (PTO) system aimed at reducing potential loads on mooring lines and support structures, thereby potentially decreasing LCoE for point absorber WECs. The presented operational principle is based on the specific classical (non-quantum) version of Fano resonance (Tribelsky, 2014), rather than the traditional Lorentzian resonance typically associated with point absorber WECs.

While Fano resonance has various applications and manifestations in atomic physics, optics, and plasmonics, this article focuses on a simplified physical model represented by two pendulums connected by a spring, as illustrated in Fig. 1. The mathematical framework for

☆ This work was supported by Science Foundation Ireland (SFI), Ireland under Grant number 20/US/3687 and 12/RC/2302_P2 (MaREI, the SFI Research Centre for Energy, Climate and Marine), and supported in part by a research grant from SFI and the Sustainable Energy Authority of Ireland under SFI-IRC Pathway Programme 22/PATH-S/10793.

☆☆ The authors are grateful to members of the Centre for Ocean Energy Research, Maynooth University, Ireland, Prof. Kush Bubbar from the University of New Brunswick, Canada, and Prof. Y. Stepanyants from University of Southern Queensland, Australia, for valuable advice and discussions.

* Corresponding author.
E-mail addresses: andrei.ermakov@mu.ie (A.M. Ermakov), jlrbutcher@gmail.com (J.L. Rose-Butcher), john.ringwood@mu.ie (J.V. Ringwood).
URL: http://coer.maynoothuniversity.ie/ (J.V. Ringwood).

https://doi.org/10.1016/j.apor.2024.104276
Received 20 April 2024; Received in revised form 10 October 2024; Accepted 12 October 2024
Available online 25 October 2024

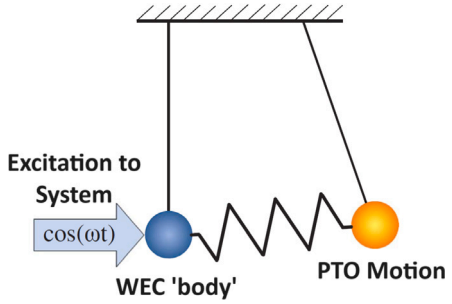

Fig. 1. A classic example of Fano resonance, with extension to the WEC case (based on Tribelsky, 2014).

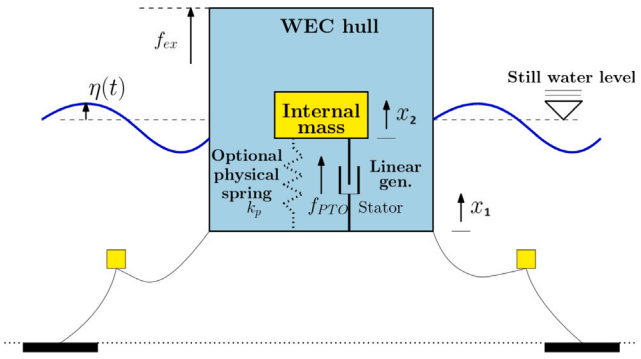

Fig. 2. A diagram of a 2-body loosely moored WEC with oscillating internal mass (Guo and Ringwood, 2021b), which is a minimal system to achieve Fano resonance.

this system and the occurrence of Fano resonance has been thoroughly examined in Rabinovich and Trubetskov (1989), Tribelsky (2014).

While the first pendulum influenced by a periodic excitation can be relatively immovable or oscillates with a small amplitude at a certain frequency, the second one can experience large-amplitude oscillations at the same frequency. The dynamic damping effect can be used, in particular, to suppress dangerous vibrations. As an example, we can mention its application to reduce the rolling of a ship in stormy oceans. As mentioned in Rabinovich and Trubetskov (1989), a certain volume of a ship (slosh) tank is filled with water to such a level that the frequency of water oscillation in the tank becomes approximately equal to the frequency of the beat of the waves on the ship. Then the rocking of the ship itself is considerably reduced, whereas water oscillation in the tanks can be significant. Applied to point absorber WECs, this translates to a buoy that remains relatively stationary in waves, coupled with significant, rapid, fluctuations of an internal translator in a linear generator, which is connected with the buoy by a spring. While other 2-body devices, with alignment of hydrodynamic and PTO degrees of freedom, have been analysed in the literature (Guo and Ringwood, 2021b), to the best of the authors' knowledge, such a system has not been considered from a Fano-resonance (i.e. wave transmitter) perspective before.

Such a conceptual operational principle for WECs has the potential to address persistent challenges in wave energy absorption:

(a) Limiting the displacement of the point absorber WEC hull in waves, using only the internal PTO response, would yield numerous advantages. These include diminished loads on WEC structures, mooring lines and anchors, resulting in reduced fatigue. This will lead to a possibility to reduce the number of mooring lines and anchors, as well as simplify their design and material. It is also likely to reduce the frequency of scheduled and unscheduled maintenance. Consequently, this would lead to lower capital and, potentially, operational costs, for WECs.

(b) One perennial difficulty is the maintenance of WECs at sea. Since WECs are typically deployed in wave-active areas, dealing with personnel transfer to an actively moving device is challenging. With reduced hull motion, personnel transfer weather windows may be broadened, increasing the opportunities for maintenance.

(c) This study suggests the imposition of constraints to limit the fluctuations of the point absorber hull, which optimally transmits wave excitation energy to the PTO system which, in turn, resonates within the WEC hull. This limited fluctuation of the WEC hull also fits well within conventional mathematical model assumptions for WECs, which are typically grounded in the linear hydrodynamic premises of Cummins' equation (Cummins, 1962), assuming that the WEC hull undergoes small displacement from equilibrium. Such an approach offers added advantages of realistically implementing various developed control strategies (Ringwood et al., 2023a,b).

The content of the subsequent sections of this article is as follows: In Section 2, the authors introduce mathematical models for a 2-body loosely-moored WEC with an oscillating internal mass, and a single-body ocean bed-referenced WEC. Section 3 is dedicated to the statement of the WEC optimisation problem. In Section 4, the outcomes of the modelling and optimisation approaches are presented and discussed. Here, Sections Section 4.1,4.2,4.3 are devoted to the derivation of the optimal parameters of the internal PTO system to achieve Fano resonance. Section 4.4 concerns the optimisation of the cylindrical buoy hull and PTO system dimensions for maximum device efficiency. The discussion and comparison of the results obtained for ocean bed-referenced and self-referenced WECs is presented in Section 5. The Conclusions section (Section 6) discusses the results obtained, as well as the feasibility and benefits of Fano resonance in wave energy conversion.

2. Mathematical models

2.1. Two-body loosely moored self-referenced WEC with an internal pto.

The application of Fano resonance to wave energy conversion can be illustrated with a 2-body loosely-moored WEC with oscillating internal mass, as illustrated in Guo and Ringwood (2021b), see Fig. 2. The internal mass m_p moves somewhat independently of the hull,where the hull and internal mass are connected by a linear generator (LinGen, converting the useful energy) and an optional physical spring k_p. Note that the LinGen could also provide a (variable) virtual spring effect k_c, though it may be more economical to use a fixed physical spring. The system extracts power through the electromagnetic damping of a linear generator d_c.

Although the mathematical model for the self-referenced WEC proposed in Guo and Ringwood (2021b) has been extensively studied in several publications focused on the development of optimal control and design for such devices (Chen et al., 2023a,b; Guo and Ringwood, 2021a), experimental validation of this model is still pending. To the best of the authors' knowledge, a similar model and device were validated in Kong et al. (2019). In addition, individual models for wave-body interactions (Cummins, 1962) and vibro-impact PTO (Ibrahim, 2009) were validated some time ago and are widely utilised.

The present study addresses a one hydrodynamic degree-of-freedom problem, limiting displacements to the heave direction. The oscillation of a heaving buoy WEC in waves is traditionally modelled by Cummins' equation (Cummins, 1962):

$$\left(M_h + M_\infty\right)\ddot{x}_1(t) + \int_0^t \dot{x}_1(\tau) k_r(t-\tau)d\tau + d_h\dot{x}_1(t) + k_s x_1(t) = f_{ex}(t) + f_{pto}(t), \quad (2)$$

where $x_1(t)$ represents the vertical position of the buoy, M_h is the mass of the buoy hull (which also includes the LinGen stator), M_∞ denotes the added-mass at infinite frequency, $k_r(t)$ is the radiation damping

impulse response function, k_s refers to the hydrostatic stiffness, d_h to (linearised) viscous water damping effects, $f_{ex}(t)$ to the wave excitation force, and $f_{pto}(t)$ describes the force applied by the PTO system.

In terms of the internal system dynamics, the position $x_2(t)$ of the LinGen translator can be described by:

$$m_p\ddot{x}_2(t) = -f_{pto}, \tag{3}$$

and

$$f_{pto} = f_{gen} + k_p[x_2(t) - x_1(t)], \tag{4}$$

where m_p represents the internal system mass of the LinGen translator and internal mass, k_p is the stiffness of the (optional) physical spring, and f_{gen} is the force generated by the linear generator.

The electrical generator can be modelled using the traditional mass–spring-damper model (Ahamed et al., 2022). Thus, we select f_{gen} to have the following components:

$$\begin{aligned} f_{gen}(t) \;=\; & k_c\,[x_2(t) - x_1(t)] + d_c\,[\dot{x}_2(t) - \dot{x}_1(t)] \\ & + m_c\,[\ddot{x}_2(t) - \ddot{x}_1(t)], \end{aligned} \tag{5}$$

where m_c and k_c are virtual mass and spring parameters respectively, and d_c is the damping parameter.

The complete dynamics of the internal mass can be described by the following equation:

$$\begin{aligned} m_p\,\ddot{x}_2(t) \;=\; & (k_p + k_c)[x_1(t) - x_2(t)] + d_c\,[\dot{x}_1(t) - \dot{x}_2(t)] \\ & + m_c\,[\ddot{x}_1(t) - \ddot{x}_2(t)]. \end{aligned} \tag{6}$$

It is important to note that in the case under study, the PTO does not include any reactive forces from either the ocean floor or any supporting marine structures.

The solution to the system described by Eqs. (2)–(6) can be determined in the frequency domain under the following assumptions:

$$x_1(t) = X_1(\omega)e^{\mathbb{j}\omega t}, \qquad x_2(t) = X_2(\omega)e^{\mathbb{j}\omega t}, \tag{7}$$

$$f_{ex}(t) = F_{ex}(\omega)e^{\mathbb{j}\omega t}, \tag{8}$$

where $X_1(\omega)$ and $X_2(\omega)$ denote the response amplitude operators (RAO) for the heaving buoy and the translator, respectively, and $F_{ex}(\omega)$ represents the excitation force to wave frequency ω response.

The solution to the Cummins Eq. (2) for a body in waves can be obtained in the frequency domain using a boundary element method (BEM) based software such as Ansys AQWA (2015). The obtained solutions for the heaving buoy hull RAO $X_1(\omega)$ for each particular frequency of a regular wave can be expressed as a ratio of to the forces $F_{ex}(\omega)$ and $F_{pto}(\omega)$ that act on it, and product of intrinsic impedance of the buoy hull $Z_{hull}(\omega)$ (Falnes, 2002) and $\mathbb{j}\omega$:

$$X_1(\omega) = \frac{F_{ex}(\omega) + F_{pto}(\omega)}{\mathbb{j}\omega Z_{hull}(\omega)}, \tag{9}$$

where

$$F_{pto}(\omega) = [(k_c + k_p) + \mathbb{j}\omega d_c - \omega^2 m_c][X_2(\omega) - X_1(\omega)], \tag{10}$$

$$Z_{hull}(\omega) = B(\omega) + \mathbb{j}\omega\left[M_h + M_a(\omega) + M_\infty - \frac{K_s}{\omega^2}\right]. \tag{11}$$

where $B(\omega)$ is the radiation resistance, K_s is the hydrostatic stiffness, M_h is the mass of the buoy hull, $M_a(\omega)$ is the added mass after the singularity at infinite frequency (M_∞) is removed.

From the equation for the PTO force (10), we can identify the intrinsic impedance of the PTO system:

$$Z_{pto} = -\frac{\mathbb{j}}{\omega}[(k_c + k_p) + \mathbb{j}\omega d_c - \omega^2 m_c]. \tag{12}$$

It is clear, from (12), that the imaginary part of Z_{pto} can be manipulated by either k_c, k_p, or m_c, while the real part depends only on d_c. Thus, the physical spring k_p between buoy hull and internal mass can, if desired, be simulated by the PTO system by manipulation of k_c. The final decision as to how to balance these parameters is based on economic considerations related to a minimum cost solution. However, it should be borne in mind that even though it may be cheaper to utilise predominantly physical mass and spring than implement through f_{gen}, the virtual quantities can be continuously adapted to cater for, for example, sea state changes.

The RAO of the heaving buoy hull $X_0(\omega)$, free from internal mass but still having the same submergence, can be determined as:

$$X_0(\omega) = \frac{F_{ex}(\omega)}{\mathbb{j}\omega Z_{hull}(\omega)}. \tag{13}$$

This parameter will be used later to illustrate the resonant frequency of the buoy hull.

The equation for the translator (3), in the frequency domain, takes the following form:

$$m_p\,\omega^2 X_2(\omega) = F_{pto}(\omega). \tag{14}$$

Then, in the frequency domain, the solution to the system described by Eqs. (9) and (14), for the RAOs of the buoy and the translator, respectively, is given by:

$$X_1(\omega) = \frac{F_{ex}(\omega)}{\Delta}[Z_{pto}(\omega) + \mathbb{j}\,m_p\,\omega], \tag{15}$$

$$X_2(\omega) = \frac{F_{ex}(\omega)}{\Delta}Z_{pto}(\omega), \tag{16}$$

where

$$\Delta = \omega\,[\mathbb{j}\,Z_{pto}(\omega)Z_{hull}(\omega) - m_p\,\omega\,(Z_{pto}(\omega) + Z_{hull}(\omega))]. \tag{17}$$

The time-averaged power, produced by the linear generator of the described system, can be evaluated as:

$$P(\omega) = Re[Z_{pto}]\,|V_2(\omega) - V_1(\omega)|^2/2, \tag{18}$$

where $V_2(\omega) = \mathbb{j}\omega X_2(\omega)$ is the velocity of the translator, and $V_1(\omega) = \mathbb{j}\omega X_1(\omega)$ is the velocity of the heaving buoy.

It can be analytically demonstrated, by solving the problem of maximising the power functional $P(\omega)$ in partial derivatives with respect to the two variables $Re[Z_{pto}]$ and $Im[Z_{pto}]$, that maximum power production can be achieved under the following unconstrained condition:

$$\begin{aligned} Z_{pto} = & \frac{m_p^2\omega^2\,Re[Z_{hull}]}{Re[Z_{hull}]^2 + \left(Im[Z_{hull}] + m_p\omega\right)^2} \\ & -\mathbb{j}\frac{m_p\omega\left(Re[Z_{hull}]^2 + Im[Z_{hull}]\left(Im[Z_{hull}] + m_p\omega\right)\right)}{Re[Z_{hull}]^2 + \left(Im[Z_{hull}] + m_p\omega\right)^2} \end{aligned} \tag{19}$$

The solution obtained corresponds to the impedance matching strategy proposed in Bacelli and Coe (2021). However, this optimal control solution does not account for the natural limitations imposed by the buoy hull and internal mass displacement. These issues are addressed in the following sections.

2.2. A single body ocean bed referenced wec.

To evaluate the efficiency of the 2-body loosely moored WEC concept and determine whether a heaving buoy hull should primarily act as a source or transmitter of energy for the PTO system, the authors compare the time-averaged power production of a self-referenced WEC (as depicted in Fig. 2) with that of a more traditional point absorber buoy anchored to the ocean bed (as shown in Fig. 3). The buoy hull shape and corresponding intrinsic impedance Z_{hull} are identical for both devices. The study assumes that the ocean bed-referenced WEC operates under a 'Simple and Effective' (SE) controller (Fusco and Ringwood, 2013), representing a constrained modification of the traditional complex conjugate (CC) control (Falnes, 2002), with instantaneous

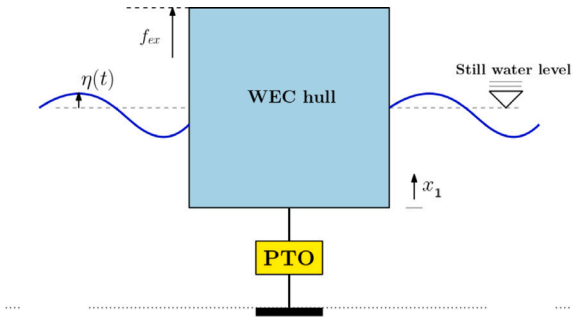

Fig. 3. A diagram of a single body ocean bed referenced WEC (Fusco and Ringwood, 2013).

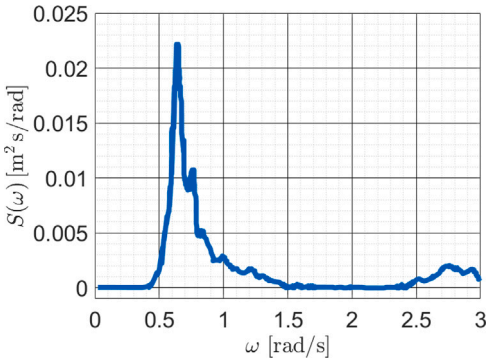

Fig. 4. Wave spectrum of a sample data set for Galway Bay, Ireland, analysed in Fusco and Ringwood (2010).

frequency tracking. However, the frequency tracking aspect of the SE controller is not utilised in this study.

In the SE method applied to the ocean bed-referenced WEC, the intrinsic impedance of the PTO system $Z^*_{pto}(\omega)$ is evaluated from the following relation:

$$Z^*_{pto}(\omega) = (2\alpha - 1)Re[Z_{hull}(\omega)] - \mathbb{j}\, Im[Z_{hull}(\omega)], \tag{20}$$

where α represents a tuning PTO damping parameter, which permits implementation of constraints on the buoy hull displacement magnitude $|\tilde{X}_1|$. Consequently, when $\alpha = 1$, the traditional CC solution is obtained.

The corresponding RAO of $\tilde{X}_1(\omega)$ and velocity $\tilde{V}_1(\omega)$ of the ocean bed-referenced WEC buoy hull can be determined using the following equations:

$$\tilde{V}_1(\omega) = \frac{F_{ex}(\omega)}{Z_{hull} + Z^*_{pto}} = \frac{F_{ex}(\omega)}{2\,\alpha\, Re[Z_{hull}(\omega)]}, \tag{21}$$

and

$$\tilde{X}_1(\omega) = \tilde{V}_1(\omega)/(\mathbb{j}\,\omega). \tag{22}$$

It is clear that an increase in the tuning parameter α results in a decrease in both the magnitudes of displacement and velocity of the buoy. The parameter α can be determined based on a maximum displacement magnitude constraint $|\tilde{X}_1| < \tilde{X}_1^{Max}$.

The time averaged power production $\tilde{P}(\omega)$ in the frequency domain (Falnes, 2002), due to the constrained displacement magnitude $|\tilde{X}_1(\omega)|$, can be evaluated as:

$$\tilde{P}(\omega) = \frac{1}{2} Re[Z^*_{pto}(\omega)]|V_1(\omega)|^2 = \frac{(2\alpha - 1)|F_{ex}(\omega)|^2}{8\,\alpha^2\, Re[Z_{hull}(\omega)]}. \tag{23}$$

It is also clear, (from (23)) that maximum power generation is attained with the optimal buoy hull displacement magnitude, occurring when $\alpha = 1$. Consequently, any decrease in the buoy hull displacement magnitude will result in a reduction of the generated power $\tilde{P}(\omega)$.

3. Optimising various operational regimes for self-referenced WECs

The optimisation challenges in control and design of WEC systems reflect the necessity to balance many conflicting objectives. In our case, the primary objective is to maximise power production $P(\omega)$, while the secondary objective aims to minimise or restrict the displacement of the heaving buoy hull $|X_1|$. In the case of a self-referenced WEC, these conflicts could potentially be resolved by introducing different control strategies that can be implemented in various sea states. In this article, the authors study and optimise various potential operational strategies for a self-referenced WEC, targeting different goals. The solution and analysis of various control optimisation problems allow us to study the fundamental properties and aid in the optimal design of the self-referenced WEC.

The first operational regime optimisation problem studies the constrained power maximisation problem $P(\omega) \rightarrow$ Max, where the limitation of the buoy hull displacement magnitude can be expressed as a rigid constraint $|X_1| < X_1^{Max}$. This constraint prevents the mooring lines from influencing the power generation process, ensuring that device stabilisation is solely achieved through the internal PTO system. An additional inherent constraint is the necessity to maintain the internal mass displacement magnitude within the structural limits of the buoy height h_c, ensuring $|X_2 - X_1| < h_c/2$.

The second operational regime optimisation problem studies the minimum achievable displacement magnitude for the self-referenced WEC, $|X_1(\omega)| \rightarrow$ Min. It is clear that the reactive force from the internal PTO is limited, so an assessment of its capability to minimise the buoy hull displacement magnitude needs to be conducted.

The range of potential solutions, balancing the first and second objectives, can be illustrated using a Pareto front. However, compared to the ocean bed-referenced WEC, the Pareto front for the self-referenced WEC has a complex shape, with a range of potentially equal local maxima due to the non-linearity of the governing equations ((15), (16)).

The implementation and optimisation of the proposed control strategies can be achieved by optimising the PTO responses Z_{pto}, and/or by optimising the buoy hull design Z_{hull}, and/or internal mass m_p values. However, an increase in buoy hull size Z_{hull}, installation of heavy internal mass, and/or PTO capable of supplying significant forces Z_{pto} could potentially significantly increase the CapEx and OpEx of the device. Thus, their unlimited increase will not help in LCoE minimisation (1).

It is evident that satisfying all objectives simultaneously is a challenging problem. Moreover, quantifying the costs of variables and functions is complex. Hence, the authors limit the presented results to illustrate specific scenarios and derive the key inter-dependencies between objectives. The optimal solution presented either targets a singular goal or presents the range of possible solutions via figures and tables to navigate conflicting objectives.

The conducted research is based on an analysis of a regular wave frequency response, which enables the identification of the fundamental system properties and provides clear illustration of the required PTO and buoy hull parameters for limitation of the buoy hull displacement magnitude and power production maximisation. While it can be argued that regular waves do not fully capture the panchromatic nature of the ocean climate, various studies have demonstrated that certain sea states can be approximated by a narrow-banded spectral process (Fusco and Ringwood, 2010). In addition, for WEC simulation studies, the (polychromatic) superposition of monochromatic waves is the common route to panchromatic analysis.

An example narrow-banded sea state is presented in Fig. 4, which illustrates real observations of wave spectra measured by an Irish

Marine Institute data buoy, located at Galway Bay on the West Coast of Ireland (53° 13′ N, 9° 18′ W, water depth nearly 20 m) (Fusco and Ringwood, 2010). Optimisation of the different operational regimes for various self-referenced WECs is conducted for regular waves with various frequencies in the range $0 < \omega < 3$ rad/s and a wave height of $H = 1$ m, allowing for study of the frequency-specific behaviour of the system. A particular emphasis is placed on waves with a period of $T_0 = 8$ s or a frequency of $\omega_0 = 0.785$ rad/s, positioned between the mean and median values (Fig. 4).

The conducted optimisation study of the resonance of the proposed WEC concept is based on the analytical solutions ((15), (16)) and performance metrics ((18), (23)) from Section 2. The variables of the optimisation process include the structural properties of a heaving buoy hull (for example, radius r_c, height h_c, draft h_d, and mass M_h for a cylindrical buoy hull) as well as internal PTO properties such as the internal mass m_p value and the intrinsic impedance Z_{pto} of a linear generator.

The stated nonlinear optimisation problems have been programmed and solved in Python using the simplicial homology global optimisation (Endres et al., 2018) and differential evolution (Storn and Price, 1997) methods, both available in the Python optimisation and root-finding library, (Scipy.Optimize, 2024). The required intrinsic impedance $Z_{hull}(\omega)$ and excitation force $F_{ex}(\omega)$ frequency responses were obtained using Capitaine (Ancellin and Dias, 2019) and Ansys AQWA (Ansys AQWA, 2015).

4. Control and design optimisation for self-referenced WECs

This section considers the set of optimisation problems that characterise the proposal of a two-body WEC system as an *energy transmitter* via Fano resonance. It will be seen that a number of these sub-problems have conflicting objectives (e.g. minimising hull motion but maximising energy capture), therefore presenting a true multi-criterion optimisation problem. The related set of problems constitute a genuine control co-design challenge, where specific physical design attributes ultimately determine the success (or otherwise) of the overall Fano objective, but are implicitly interwoven with the constrained control design problem.

4.1. Case 1: Optimal constrained control solution

The first case study is dedicated to solution of the optimal constrained control problem for a WEC with the self-referenced WEC system. We consider a semi-submerged cylindrical buoy with radius $r_c = 3$ m, height $h_c = 6$ m, draft $d_c = 3$ m, hull mass $M_h = 68{,}040$ kg and water depth 200 m. The initially selected internal mass is $m_p = 17{,}010$ kg, which is 20% of the overall mass of the whole device M_c. The intrinsic impedance $Z_{hull}(\omega)$ and excitation-force $F_{ex}(\omega)$ frequency responses for the cylindrical hull, calculated using Ansys AQWA (2015), are depicted in Fig. 5.

In most of the published research, e.g. Guo and Ringwood (2021b), Chen et al. (2023a), the internal spring value k_p is considered as constant, and control is implemented solely by adjusting the PTO damping coefficient d_c (Chen et al., 2023a). In this research, the authors consider a linear generator, which has the capability to simulate also variable 'virtual' spring k_c and mass m_c controller parameters (4). While the objective is to maximise power generation (18) by optimising Z_{pto} parameters, it is also required that the displacement magnitude of the heaving buoy hull remains relatively small $|X_1| < 1$ m. In addition, the relative displacement magnitude of the generator translator is restricted by the buoy height, while remaining adequate for power generation $0.5 < |X_2 - X_1| < 3$ m. Thus, a constrained optimisation problem, written in the following form,

$$|X_1| < 1 \text{ m}, \quad 0.5 < |X_2 - X_1| < 3 \text{ m}, \quad P(\omega) \to \text{Max}, \tag{24}$$

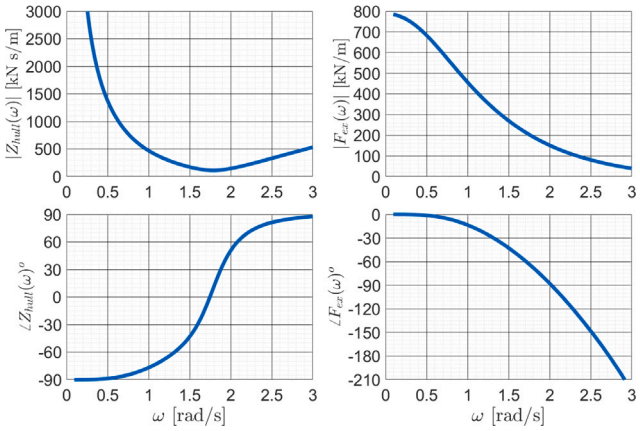

Fig. 5. Intrinsic impedance $Z_{hull}(\omega)$ and excitation force $F_{ex}(\omega)$ frequency responses for the cylindrical buoy with dimensions: $r_c = 3$ m, $h_c = 6$ m, and $h_d = 3$ m, computed using Ansys AQWA (2015).

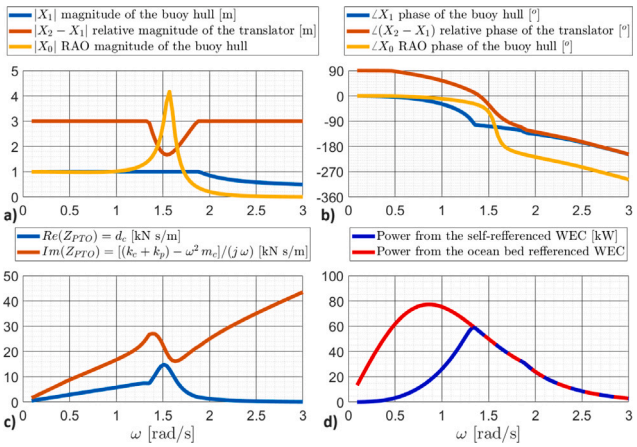

Fig. 6. Power production optimisation (see Eq. (24)) in the frequency domain for a self-referenced WEC with cylindrical hull parameters $r_c = 3$m, $h_c = 6$m, $h_d = 3$m and $m_p = 0.2M_c$: (a) optimal displacements of the hull and internal mass, as well as RAO operator magnitude for the hull, (b) their phases, (c) required Z_{pto} parameters, (d) comparison of power generation between the self-referenced and ocean bed-referenced WECs, operating with the same buoy hull displacement magnitude.

is solved. The solution to this problem, which comprises the optimal displacement magnitudes and phases of the buoy hull $|X_1|$ and internal mass $|X_2 - X_1|$, as well as the optimal PTO parameters $Z_{pto}(\omega)$ and power production $P(\omega)$ for a range of wave frequencies ω, is presented in Fig. 6. In addition, the response amplitude operator, as per Eq. (13) (indicated by the yellow line), is depicted to illustrate the resonant frequency of the selected cylindrical hull.

Fig. 6a demonstrates that the internal mass predominantly operates at the upper limit of its allocated amplitude constraint, with an exception near the cylindrical hull resonant frequency, at $\omega = 1.6$ rad/s, where maximum energy extraction is achieved, with $P = 60$ kW. This displacement magnitude reduction aligns with inflections in the PTO parameters (Fig. 6c). The translator and buoy hull exhibit relative quarter-phase fluctuations (90°) with each other for low wave frequencies until the buoy's resonant frequency (Fig. 6b). Beyond resonance, their movements shift to being in-phase.

The comparison of power generation by the self-referenced and ocean-bed-referenced WECs is shown in Fig. 6d. Both WEC systems adhere to the same displacement magnitude $|X_1|$ profile for the buoy hull, as depicted in Fig. 6a (blue line). In all scenarios, the shape of the heaving buoy is consistent. It is evident that the ocean bed-referenced WEC can generate more power when $\omega < 1.3$ rad/s. However, the

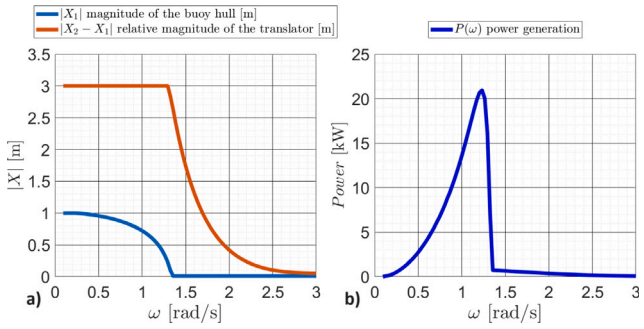

Fig. 7. (a) Minimum achievable buoy hull displacement magnitude for the cylindrical WEC with $r_c = 3$ m, $h_c = 6$ m, $h_d = 3$ m and $m_p = 0.2M_c$ with the internal PTO systems, across various wave frequencies; (b) Corresponding power generation.

control of ocean bed-referenced WEC would require a significant reactive force, causing substantial loading on the anchoring and mooring structure. The installation of such rigid ocean bed-based structures will significantly increase the LCoE of generated power (1). At the same time when $\omega > 1.3$ rad/s, the self-referenced WEC has the same performance as the ocean bed referenced WEC that utilises "simple and effective" control and follows the same displacement magnitude $|X_1|$. This implies that the optimum power transmission has been parametrically achieved, with the heaving buoy hull functioning as a transmitter of wave energy whilst resonance is realised within the internal PTO system. However, for the targeted frequency $\omega_0 = 0.785$ rad/s, the power production for the self-referenced WEC is $P(\omega_0) = 13.5$ kW, which is significantly lower than the power produced by the ocean bed-referenced WEC $\tilde{P}(\omega_0) = 76$ kW when operating under the same displacement constraint of $|X_1| < 1$ m.

4.2. Case 2: Minimisation of hull displacement

The second case study analyses the minimum displacement magnitude $|X_1(\omega)|$ which can be achieved with the internal PTO system for the presented in the previous Section 4.1 cylindrical buoy hull WEC, for various wave frequencies ω.

The minimum achievable displacement magnitude of the buoy hull $|X_1(\omega)|$, and corresponding power generation $P(\omega)$, as a function of wave frequency ω are illustrated in Fig. 7. Clearly, the considered internal mass and PTO cannot completely restrict the buoy hull displacements (i.e. $|X_1| = 0$) for frequencies below 1.3 rad/s. However, the traditional (ideal) Fano resonance effect is achieved when $\omega > 1.3$ rad/s, where the displacement of the buoy hull is almost zero (blue line), but the internal mass fluctuates inside the hull with significant amplitude (red line), though the power production for such an operational regime is relatively small.

Thus, complete restriction of the buoy hull displacement magnitude ($|X_1| = 0$) will result in virtually no power production, despite significant fluctuation of the heavy internal mass. Nevertheless, it has been demonstrated that it is possible to constrain the position of the buoy hull using only the internal response of the PTO, without the need for mooring lines or supporting marine structures (assuming no external drift forces).

4.3. Case 3: Optimisation of internal mass and overall device mass ratio

This third case study focuses on a parametric analysis concerning the optimal ratio between the internal and overall device masses m_p/M_c, and the corresponding optimal constrained control solutions. The sum of the hull mass M_h and internal mass m_p – the overall device mass M_c – is considered fixed. Thus, the equilibrium semi-submerged position of the device will remain the same, regardless of changes in the ratio m_p/M_c. The same cylindrical buoy hull WEC design as in

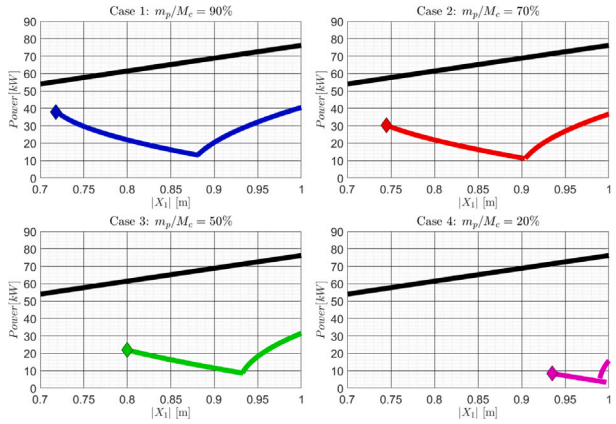

Fig. 8. The relationship between the power production and buoy hull displacement magnitude $|X_1|$, for ocean bed reference device (black line), and self-referenced devices (colour lines) for various cases of the relative ratio of the internal mass to the overall mass of the system m_p/M_c. (The results are obtained for a cylindrical WEC with $r_c = 3$ m, $h_c = 6$ m, and $h_d = 3$ m).

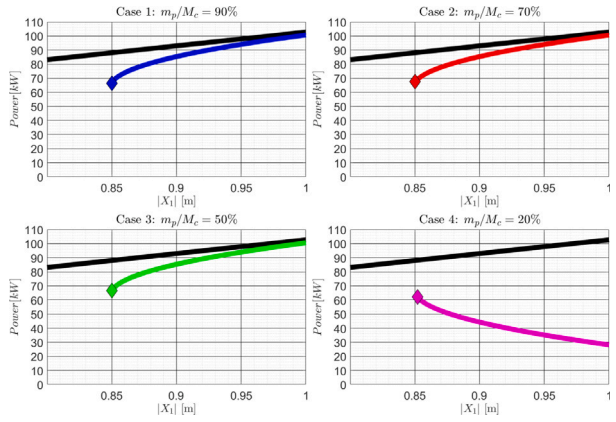

Fig. 9. The relationship between the power production and buoy hull displacement magnitude $|X_1|$, for ocean bed reference device (black line), and self-referenced devices (colour lines) for various cases of the relative ratio of the internal mass to the overall mass of the system m_p/M_c. (The results are obtained for a cylindrical WEC with $r_c = 4$ m, $h_c = 8$ m, and $h_d = 6.4$ m).

Section 4.1 (with with $r_c = 3$ m, $h_c = 6$ m, $h_d = 3$ m and $M_c = 85$ tonnes), and a larger buoy with $r_c = 4$ m, $h_c = 8$ m, $h_d = 6.4$ m and $M_c = 322$ tonnes, are examined.

For this analysis, the selected regular wave with $\omega_0 = 0.785$ rad/s and $H = 1$ m is considered. By varying the internal mass value m_p, we aim to evaluate the trade-off between the magnitude of the buoy hull displacement $|X_1|$ and power generation $P(\omega)$.

Fig. 8 illustrates the range of solutions obtained for the original smaller hull, satisfying the conditions $|X_1| < 1$ m and $0.5 < |X_2 - X_1| < 3$ m, for various cases of the relative ratio of the internal mass m_p to the overall mass of the system M_c (indicated by different colours). The minimum achievable displacement magnitude for the self-referenced device is highlighted with the diamond symbol ◇. The black reference line represents the power produced by a bottom-referenced device operating with the same displacement magnitude.

It can be observed in Fig. 8 that the solutions for the self-referenced device correspond to the intersection of two curves, underscoring the non-linearity of the optimisation problem. This arises from the fact that, for a two-body device, optimisation is required for both the real and imaginary components of the intrinsic impedance of the PTO system (see Eqs. (15)–(19)). Consequently, it is possible to obtain more than one power production solution for the same displacement

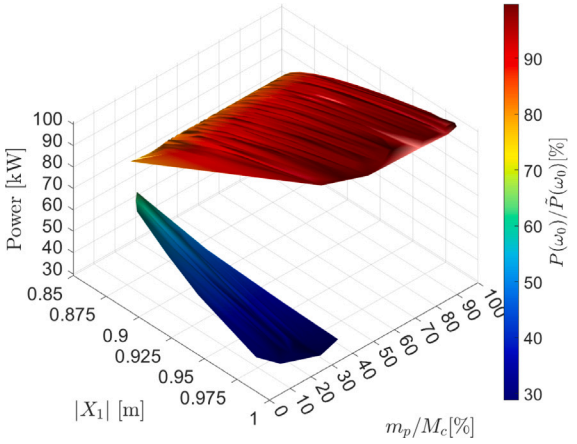

Fig. 10. The relationship between the power produced by a self-referenced WEC, the displacement of the buoy hull $|X_1|$, and the ratio between internal mass and overall mass of the device m_p/M_c. The ratio of energy from the self-referenced device to the bottom-referenced device, operating with the same buoy hull displacement magnitude $|X_1|$ is highlighted using colour scheme. (The results are obtained for a cylindrical WEC with $r_c = 4$ m, $h_c = 8$ m, and $h_d = 6.4$ m).

value. This issue of identifying the global maximum is addressed by applying optimisation methods such as simplicial homology (Endres et al., 2018) or differential evolution (Storn and Price, 1997). In contrast, for a bottom-referenced device, the imaginary component of the PTO is always cancelled by the chosen simple and effective control strategy (21). Therefore, it can be concluded that the real-time control implementation for a self-referenced device will require solving non-linear equations and selecting the optimal solution at each time step, necessitating supervisory control.

Fig. 8 shows that, when comparing Case 1 to the other presented cases, minimising the buoy hull displacement magnitude or maximising the generated power requires a substantial internal mass, with $m_p/M_c = 90\%$. However, the generated power is significantly lower compared to the power that could be produced by a bottom-referenced device. This suggests that the installed internal mass and its fluctuation magnitude are insufficient to achieve comparable power production at the considered wave frequency. Therefore, an adjustment to the buoy hull design is necessary.

The results presented in Fig. 9 are obtained for a much larger device with dimensions $r_c = 4$ m, $h_c = 8$ m, and $h_d = 6.4$ m, which can accommodate a much heavier mass and allow for a larger fluctuation magnitude. The presented solutions satisfy the conditions $|X_1| < 1$ m and $0.5 < |X_2 - X_1| < 4$ m. It is visible from Fig. 9 Cases 1, 2, and 3 that the performance of the self-referenced device is very close to that of the bottom-referenced device operating with the same displacement magnitude. However, in Case 4, the internal mass is not sufficient to reproduce the optimal control solutions from the previous cases.

The complete set of solutions for the case of the large hull, depicting the relationship between the power output of a self-referenced WEC, the displacement of the buoy hull $|X_1|$, and the internal-to-overall mass ratio of the device m_p/M_c, is shown in Fig. 10. The plot reveals that the solution set forms two surfaces, emphasising the non-linearity of the optimisation problem. The ratio of energy produced by the self-referenced device compared to a bottom-referenced device, both operating with the same buoy hull displacement magnitude $|X_1|$, is represented by the colour scheme. Thus, it can be concluded that maximisation of power production, or minimisation of the buoy hull displacement, for a self-referenced WEC will require installation of a significant internal mass.

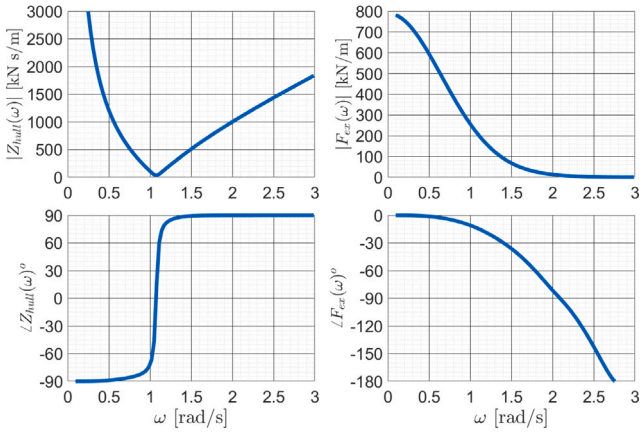

Fig. 11. Intrinsic impedance Z_{hull} and excitation force F_{ex} frequency responses for a cylindrical WEC with $r_c = 5$ m, $h_c = 9$ m and $h_d = 7.2$ m, computed using Ansys AQWA (2015).

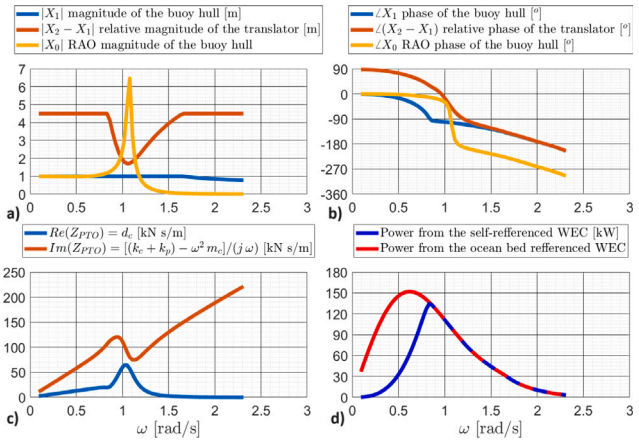

Fig. 12. Power production optimisation (Eq. (25)) in the frequency domain for a self-referenced WEC with cylindrical hull $r_c = 5$m, $h_c = 9$m, $h_d = 7.2$ m and $m_p = 0.2M_c$: (a) optimal displacement of the hull and internal mass, as well as RAO operator magnitude for the hull, (b) their phases, (c) required Z_{pto} parameters, (d) comparison of power generation between the self-referenced and ocean-bed-referenced WECs, operating with the same buoy hull displacement magnitude.

4.4. Case 4: Optimisation of cylindrical buoy hull dimensions

Another method to enhance power extraction at low wave frequencies, for a self-referenced WEC, while using a minimal internal mass, is to modify the design of the buoy hull.

This subsection focuses on determining the optimal dimensions of a cylindrical heaving buoy hull for a self-referenced WEC, which maximises power generation, $P(\omega)$, while limiting the buoy hull displacement magnitude $|X_1|$. The optimisation is conducted for the same selected regular wave with $\omega_0 = 0.785$ rad/s and $H = 1$ m. The chosen buoy hull design takes the form of a cylinder with radius r_c, height h_c, and draft h_d. The overall mass of the device $M_c = M_h + m_p$ can be determined using Archimedes' principle. The intrinsic impedance $Z_{hull}(\omega)$ and excitation force $F_{ex}(\omega)$ frequency responses for each specific combination of h_c, r_c and h_d are computed in Ansys AQWA (2015). The obtained frequency responses, $Z_{hull}(\omega)$ and $F_{ex}(\omega)$, were interpolated using a 30th order polynomial in ω.

The optimisation ranges for the buoy hull dimensions are set between $0.5 < r_c < 5$ m for radius, $3 < h_c < 8$ m for height, and draft falling between $0.4h_c < h_d < 0.8h_c$. These constraints ensure the buoy manufacturability, ease of installation, and ability to withstand oceanic conditions. The displacement magnitude of the buoy hull fluctuations is constrained such that $|X_1| < 1$ m. The transmitter mass is assumed to

Table 1
Time averaged power production [in kW] for a self-referenced WEC with radius r_c, height h_c, and drafts $h_d = 0.4h_c$ and $h_d = 0.8h_c$, evaluated for regular waves with $\omega_0 = 0.785$ s and $H = 1$ m.

Draft $h_d = 0.4\,h_c$							
$r_c \setminus h_c$	3	4	5	6	7	8	9
0.5	0.04	0.09	0.16	0.25	0.35	0.47	0.61
1	0.13	0.37	0.65	0.99	1.41	1.89	2.45
1.5	0.30	0.82	1.45	2.24	3.17	4.26	5.51
2	0.56	1.46	2.59	3.98	5.64	7.58	9.80
2.5	0.93	2.31	4.06	6.21	8.83	11.86	15.33
3	1.44	3.38	5.86	8.99	12.75	17.13	22.13
3.5	2.16	4.71	8.08	12.32	17.44	23.39	30.20
4	3.08	6.33	10.70	16.24	22.91	30.69	39.57
4.5	4.22	8.26	13.76	20.76	29.18	39.03	50.27
5	5.58	10.51	17.27	25.89	36.29	48.44	62.28

Draft $h_d = 0.8\,h_c$							
$r_c \setminus h_c$	3	4	5	6	7	8	9
0.5		0.16	0.30	0.48	0.70	0.97	1.26
1		0.60	1.19	1.92	2.81	3.85	5.03
1.5		1.31	2.64	4.29	6.29	8.67	11.32
2		2.23	4.62	7.56	11.17	15.43	20.14
2.5		3.39	7.16	11.79	17.44	24.14	31.50
3		4.74	10.21	16.97	25.17	34.85	45.40
3.5		6.38	13.83	23.09	34.34	47.60	61.82
4		8.33	18.13	30.25	45.07	62.43	80.72
4.5		10.61	23.08	38.51	57.37	79.36	101.99
5		13.34	28.73	47.88	71.30	98.41	125.47

be 20% of the overall device mass, i.e. $m_p = 0.2M_c$, while the mass of the buoy hull is $M_h = 0.8M_c$. The transmitter displacement magnitude is constrained by the hull height, i.e. $0.5 < |X_2 - X_1| < h_c/2$, but still significant.

$$|X_1| < 1 \text{ m}, \quad 0.5 < |X_2 - X_1| < h_c/2, \quad P(\omega) \to \text{Max} \tag{25}$$

The selected sample results from the solution of the cylindrical buoy hull dimension optimisation problem (25) are presented in Table 1. Table 1 shows the power production for a self-referenced WEC (with internal mass $m_p = 0.2M_c$) for various values of height h_c, draft h_d, and radius r_c, evaluated for a target wave with frequency $\omega_0 = 0.785$ rad/s and height $H = 1$ m.

It is evident that the power generated by the self-referenced WEC $P(\omega)$ increases with an increase in height h_c, draft h_d, and radius r_c of the cylindrical hull. The need for a tall cylindrical hull, for power generation maximisation, can be attributed to the space required for internal mass fluctuation. Additionally, the cylinder must be of adequate size to accommodate a substantial internal mass, and increase the wave capture diameter (relative capture width — RCW).

From Table 1, it is clear that maximum power production occurs at a boundary of the parametric space, specifically the bottom right corner. However, the introduction of an alternative performance metric, such as power/volume, would result in a shift in optimal solution towards the upper left of Table 1. Thus, optimising solely based on geometric parameters may be somewhat misleading, from a more realistic economic (e.g. LCoE) perspective, and a comprehensive economic assessment is necessary (Guo and Ringwood, 2021a). Nevertheless, Table 1 illustrates the sensitivity of power production to variations in the geometric parameters.

Maximum power generation is achieved for a cylindrical buoy hull with parameters $r_c = 5$ m, $h_c = 9$ m, and $h_d = 7.2$ m, the intrinsic impedance $Z_{hull}(\omega)$ and excitation force $F_{ex}(\omega)$ frequency responses of which are presented in Fig. 11. The optimal constrained control solutions for the selected design are illustrated in Fig. 12. It is important to note that the results shown in Fig. 12 are limited to $\omega < 2.3$ rad/s, as it is not possible to satisfy the constraints outside of this interval. The comparative power generation by the ocean-bed-based and self-referenced WECs (illustrated in Fig. 12d) for the selected buoy hull design shows that these two WECs have equal power production for a much larger wave frequency range, $\omega > 0.85$ rad/s, compared to the initial reference design (Fig. 6d), specifically $\omega > 1.3$ rad/s.

The power production by a self-referenced WEC for the targeted wave frequency $\omega_0 = 0.785$ rad/s is significant at $P(\omega_0) = 121.5$ kW. This value is only marginally less than the power generated by the ocean-bed-referenced WEC operating with the same displacement (see Fig. 12d), which is $\tilde{P}(\omega_0) = 142$ kW. This improvement can be also attributed to the resonant frequency of the selected cylinder hull being much closer to the target frequency (Fig. 12a) compared to the case of the initial reference cylinder (Fig. 6a).

5. Overall comparison between ocean bed-referenced and self-referenced WECs

This section is dedicated to a comparative qualitative comparison of the results from Section 4, with an overview presented in Table 2.

Section 4 demonstrates that the ocean-bed-referenced WEC has higher power production than the self-referenced WEC, due to its potentially unlimited reactive PTO force. However, the provision of reactive PTO force by the ocean-bed-referenced WEC will induce significant loading on the seabed anchor, potentially leading to fatigue and necessitating the installation of an expensive rigid underwater structure able to tolerate the maximum vertical PTO force. With this significant load cycling, more frequent maintenance may be required, compared to the self-referenced system, where the internal reactive PTO force imposes no loading on the mooring lines. Although the stability of the ocean-bed-referenced WEC can be easily maintained by rigid ocean bed anchoring, the control strategy proposed in this article for the self-referenced WEC naturally achieves station keeping (in the absence of external drift forces). Furthermore, it has been demonstrated that, while the displacement of the translator in a linear generator is the same as the displacement of the buoy hull for the ocean bed-referenced WEC, the displacement of the translator in the self-referenced system is limited only by the buoy hull design, which could potentially offer more options for operational regimes and power production.

Therefore, it can be concluded that despite lower power production, the self-referenced WEC will likely have lower CapEx and OpEx, potentially resulting in a lower LCoE compared to the ocean bed-referenced

Table 2
Comparison of the self-referenced and ocean bed-referenced point absorber WECs.

Ocean bed-referenced WEC	Self-referenced WEC
Potentially higher power production especially for the low frequency waves	Potentially lower power production especially for the low frequency waves
Potentially unlimited reactive PTO force	The reactive PTO force is limited with the values of the internal and buoy hull masses
In general, the displacement of the translator in the linear generator is the same as the displacement of the buoy hull	The displacement of the translator in the linear generator is independent from the displacement of the buoy hull and limited only with the buoy hull design
Requires installation of the expensive and strong seabed anchoring	Does not require strong rigid seabed anchoring
The reactive PTO force causes loadings on the seabed anchoring	The internal reactive PTO force does not cause any loadings on the mooring lines
Could require more often maintenance of seabed infrastructure due to the fatigue	May require less often maintenance
Stability of the WEC is maintained by the seabed anchoring	Stability of the WEC could be maintained by the presented control strategy
Potentially higher CapEx and OpEx	Potentially lower CapEx and OpEx

WEC. However, to achieve maximum performance, the design of the self-referenced WEC must include a significant buoy hull size, a heavy internal mass, and sufficient space for internal mass fluctuations.

6. Conclusion

The conducted research confirms the feasibility of applying a Fano resonance inspired operational principle to a self-referenced WEC. Such an operational principle is demonstrated for a minimal system, exemplified by a two-body loosely-moored self referenced WEC (Guo and Ringwood, 2021b). The developed analytical model focuses on displacements and power extraction solely in the heave direction. It is also constrained by linear theory assumptions concerning the interaction between waves and the hull structure. Within the concept of a self-referenced WEC, the heaving buoy hull is viewed as a transmitter of wave energy, where resonance is achieved internally within the PTO system.

It has been shown that a self-referenced WEC hull can more easily sustain its position in the wave solely through internal PTO action, potentially diminishing strain on mooring lines. It has also been demonstrated that the self-referenced WEC can achieve energy conversion performance similar to the ocean-bed-referenced WEC, operating under the same displacement magnitude constraint. However, to achieve the optimal operational regime, a substantial internal mass must be installed, also necessitating a reduction in the weight of the buoy hull. This operational regime could potentially reduce both the number and the material/design cost of the required mooring lines and anchors, thereby decreasing both the CapEx and OpEx for a WEC, leading to a reduction in the LCoE of renewable wave energy.

The limited displacement of the heaving buoy, for the Fano-based self-referenced WEC, also brings the additional advantage of adherence to the linear assumptions of Cummins' equation (Cummins, 1962), particularly in relation to small movements about equilibrium. While more elaborate, and higher fidelity, hydrodynamic models are available, they come at a computational cost, and do not easily lend themselves to model-based control design. While some nonlinear model-based WEC control design philosophies are available (e.g. Faedo et al. (2021)), simpler and more computationally attractive control design paradigms are usually preferable, while the literature abounds with WEC control studies based on linear model which conveniently ignore the fact that the control action itself violates one of the main assumption upon which the linear model is based (Windt et al., 2021).

The obtained optimal control solutions for self-referenced WEC illustrate a broader array of options for optimal control design compared to ocean-bed-referenced WEC systems. The showcased scatter plot emphasises the potential of finding optima for the PTO parameters, internal and buoy hull masses, as well as the displacement magnitudes of the buoy hull, and internal mass for optimal self-referenced WEC design.

The research conducted on optimising the design of cylindrical buoy hull for maximising energy extraction by self-referenced WEC, suggests that the most efficient design is a significantly submerged, large cylinder, which can accommodate a heavy internal mass and provide substantial amplitude for the internal translator fluctuations. Additionally, it is crucial that the resonant frequency of the buoy hull closely aligns with the target wave frequency, to maximise wave energy absorption. A parametric study on the internal PTO parameters uncovers significant nonlinear trends in their inter-dependencies.

One limitation of the study is that the PTO and heaving buoy hull design assessments, along with performance evaluations, are confined to the frequency domain in the heave direction only. Exploring the potential of extending the proposed operational principle to the sway and surge directions may offer additional stabilisation for the WEC, though with potentially increased PTO complexity.

The relatively simple spring/mass/damper controller employed here has limitations in relation to the power/displacement trade-off achievable. Specifically, more advanced controllers, such as MPC, or MPC-like (Faedo et al., 2017) can manage hard constraints more effectively, while fully exploiting the dynamical space within the constraints. Such considerations fall within the area of control co-design, in which integrated system/controller design takes place, recognising the dependency of the optimal device physical characteristics on the control strategy employed, and vice-versa. Some of these issues are usefully addressed for single-body and 2-body system by Liu et al. (2024).

CRediT authorship contribution statement

Andrei M. Ermakov: Writing – original draft, Methodology, Investigation, Formal analysis, Funding acquisition, Conceptualization. **Jack L. Rose-Butcher:** Writing – original draft, Investigation, Formal analysis. **John V. Ringwood:** Writing – review & editing, Supervision, Funding acquisition, Conceptualization.

Declaration of competing interest

The authors declare that they have no known competing financial interests or personal relationships that could have appeared to influence the work reported in this paper.

References

Ahamed, R., McKee, K., Howard, I., 2022. A review of the linear generator type of wave energy converters' power take-off systems. Sustainability 14 (16), 9936.
Ancellin, M., Dias, F., 2019. Capytaine: a Python-based linear potential flow solver.. J. Open Source Softw. 4 (36), 1341.
Ansys AQWA, 2015. Aqwa Theory Manual. ANSYS, Inc..
Bacelli, G., Coe, R.G., 2021. Comments on control of wave energy converters. IEEE Trans. Control Syst. Technol. 29 (1), 478–481.
Chen, S., Guo, B., Said, H.A., Yang, K., Ringwood, J.V., 2023a. Wave-to-wire modelling of a vibro-impact wave energy converter for ocean data buoys. IFAC-PapersOnLine 56 (2), 11735–11740, 22nd IFAC World Congress.
Chen, S., Zuo, Y., Yang, K., Guo, B., 2023b. A nonlinear model predictive control strategy for a wave-to-wire model of vibro-impact wave energy converters. In: 12th International Conference on Renewable Power Generation. RPG 2023, pp. 1337–1343.
CorPower Ocean, 2023. Available: https://corpowerocean.com/. (Accessed 19 April 2024).
Cummins, W., 1962. The impulse response function and ship motions. In: Symp. on Ship Theory, Schiffstechnik. pp. 101–109.
Endres, S.C., Sandrock, C., Focke, W.W., 2018. A simplicial homology algorithm for Lipschitz optimisation. J. Global Optim. 72, 181–217.
Faedo, N., Olaya, S., Ringwood, J.V., 2017. Optimal control, MPC and MPC-like algorithms for wave energy systems: An overview. IFAC J. Syst. Control 1, 37–56.

Faedo, N., Scarciotti, G., Astolfi, A., Ringwood, J.V., 2021. Nonlinear energy-maximizing optimal control of wave energy systems: A moment-based approach. IEEE Trans. Control Syst. Technol. 29 (6), 2533–2547. http://dx.doi.org/10.1109/TCST.2020.3047229.

Falnes, J., 2002. Ocean Waves and Oscillating Systems: Linear Interactions Including Wave-Energy Extraction. Cambridge University Press.

Fusco, F., Ringwood, J.V., 2010. Short-term wave forecasting for real-time control of wave energy converters. IEEE Trans. Sustain. Energy 1 (2), 99–106.

Fusco, F., Ringwood, J.V., 2013. A simple and effective real-time controller for wave energy converters. IEEE Trans. Sustain. Energy 4 (1), 21–30.

Giglio, E., Petracca, E., Paduano, B., Moscoloni, C., Giorgi, G., Sirigu, S.A., 2023. Estimating the cost of wave energy converters at an early design stage: A bottom-up approach. Sustainability 15 (8).

Guo, B., Ringwood, J.V., 2021a. Geometric optimisation of wave energy conversion devices: A survey. Appl. Energy 297, 117100.

Guo, B., Ringwood, J.V., 2021b. Non-linear modeling of a vibro-impact wave energy converter. IEEE Trans. Sustain. Energy 12 (1), 492–500.

Guo, B., Ringwood, J.V., 2021c. A review of wave energy technology from a research and commercial perspective. IET Renew. Power Gener. 15 (14), 3065–3090.

Guo, C., Sheng, W., De Silva, D.G., Aggidis, G., 2023. A review of the levelized cost of wave energy based on a techno-economic model. Energies 16 (5).

Ibrahim, R.A., 2009. Vibro-Impact Dynamics: Modeling Mapping and Applications. Springer Science and Business Media, Berlin, Germany.

Jahangir, M.H., Alimohamadi, R., Montazeri, M., 2023. Performance comparison of pelamis, wavestar, langley, oscillating water column and Aqua Buoy wave energy converters supplying islands energy demands. Energy Rep. 9, 5111–5124.

Kong, F., Su, W., Liu, H., Collu, M., Lin, Z., Chen, H., Zheng, X., 2019. Investigation on PTO control of a combined axisymmetric Buoy-WEC (CAB-WEC). Ocean Eng. 188, 106245.

Liu, J., Li, X., Yang, L., Wu, X., Huang, J., Mi, J., Zuo, L., 2024. Achieving optimum power extraction of wave energy converters through tunable mechanical components. Energy 130322.

Rabinovich, M.I., Trubetskov, D.I., 1989. Oscillations and Waves in Linear and Nonlinear Systems. Kluver Academic Publishers.

Ringwood, J.V., Tom, N., Ferri, F., Yu, Y.-H., Coe, R.G., Ruehl, K., Bacelli, G., Shi, S., Patton, R.J., Tona, P., Sabiron, G., Merigaud, A., Ling, B.A., Faedo, N., 2023a. The wave energy converter control competition (WECCCOMP): Wave energy control algorithms compared in both simulation and tank testing. Appl. Ocean Res. 138, 103653.

Ringwood, J.V., Zhan, S., Faedo, N., 2023b. Empowering wave energy with control technology: Possibilities and pitfalls. Annu. Rev. Control 55, 18–44.

Scipy.Optimize, 2024. Available: https://docs.scipy.org/doc/scipy/reference/optimize.html. (Accessed 28 August 2024).

Storn, R., Price, K., 1997. Differential evolution – a simple and efficient heuristic for global optimization over continuous spaces. J. Global Optim. 11, 341–359.

Tribelsky, M.I., 2014. Linear and Nonlinear Evolution in Time and Space. Shigemasa Printing, Yamaguchi.

Wave Star, 2023. Available: https://wavestarenergy.com/. (Accessed 14 April 2024).

Windt, C., Faedo, N., Penalba, M., Dias, F., Ringwood, J.V., 2021. Reactive control of wave energy devices–the modelling paradox. Appl. Ocean Res. 109, 102574.